JOURNAL OF SPACECRAFT AND ROCKETS
Vol. 31, No. 6, November–December 1994

Design and Structural Analysis of Highly Mobile Space Suits and Gloves

John A. Main,* Steven W. Peterson,† and Alvin M. Strauss‡
Vanderbilt University, Nashville, Tennessee 37235

This paper evaluates the factors that control the flexibility of fabric space-suit elements, in particular gloves, by examining a bending model of a pressurized fabric tube. Results from the model are used to evaluate the design strategies used in space-suit components, to evaluate the current direction in research on highly mobile space-suit gloves and to suggest changes necessary for optimum glove fabric selection. Finally it is shown that the modulus of the fabric used in space-suit joint construction is as important to the flexibility of the joint as the glove size and design.

Nomenclature

E_f = fabric fill modulus, N/m
E_w = fabric warp modulus, N/m
K = glove curvature, m^{-1}
M = applied moment, N-m
N_f = stress resultant in fabric fill, N/m
N_h = stress resultant in glove-joint hoop direction, N/m
N_l = stress resultant in glove-joint longitudinal direction, N/m
N_w = stress resultant in fabric warp, N/m
N_{wf} = shear-stress resultant in fabric, N/m
p = glove pressurization, Pa
r = radius of glove cross section, m
V_e = exhaust voltage threshold, V
V_p = pressurization voltage threshold, V
γ_{wf} = fabric shear strain
ε_f = strain in fabric fill
ε_l = strain in glove-joint longitudinal direction
ε_w = strain in fabric warp
θ = angle measured around the circumference of the glove joint
θ_0 = wrinkle half angle
ν_f = Poisson's ratio of fabric-fill
ν_h = Poisson's ratio of fabric weave corresponding to the glove-joint hoop direction
ν_l = Poisson's ratio of fabric weave corresponding to the glove-joint longitudinal direction
ν_w = Poisson's ratio of fabric warp
ρ = radius of curvature, m

Introduction

THE design of an ideal space suit and gloves and the selection of appropriate fabrics is an extremely demanding task. The resulting glove should preserve the function and utility of the hand while providing protection from the harsh environment of space. Hazards that must be addressed when designing both the space suit and gloves are extremes of heat and cold, meteoroid impact, radiation, abrasion, chemical exposure, puncture, high loads from suit pressurization, and task-induced loads. Designing for these hazards generally works against designing a comfortable and flexible suit and gloves, because greater astronaut protection generally requires more suit layers and more robust fabrics.

Received Sept. 2, 1993; revision received March 15, 1994; accepted for publication March 23, 1994.

*Research Associate, Department of Mechanical Engineering. Box 1592B.
†Assistant Professor, Department of Mechanical Engineering, Box 1592B.
‡Professor and Chairman, Department of Mechanical Engineering, Box 1592B.

Space suits have evolved from the virtually immobile when pressurized Mercury suits[1] to the advanced Shuttle suits in use today (see Fig. 1). While the current space suits represent a remarkable achievement in soft-goods design and construction, concerns still exist about the flexibility of the suit and the gloves in particular. The astronaut working inside the suit is essentially inhabiting a form-fitting pressurized fabric structure that has a characteristic neutral shape. Any movement that the astronaut performs requires an expenditure of energy to bend or deform the suit away from that neutral position. This adds to astronaut fatigue and reduces extravehicular productivity.[2]

Decreasing the stiffness and increasing the flexibility of various suit elements has been the focus of a variety of recent investigations. These have focused on evolutionary changes in suit component design through a trial-and-error design process. Recent developments in the literature include the results of a design competition to produce the next generation of space-suit gloves that resulted in modified designs for gloves,[3] an automated glove sizing and production method based on three-dimensional laser scanning techniques,[4] and changes in fabric pattern easements and bearing friction to improve joint mobility.[5] All of this previous research relied upon experience gained over long periods of time working in this very specialized design area to improve the space suit and gloves. While experience is invaluable, the development of a rational structural model for fabric space-suit components is also needed to improve insight into the problem of suit stiffness and to establish design parameters.

This paper focuses on the development of such a model and utilizes it to predict the effect that changes in space-suit pressurization, size, and fabric mechanical properties have on suit mobility and dexterity, and glove mobility in particular. The approach taken here is based on first developing a model for the bending behavior of an inflated fabric space-suit joint. Then simulations are performed to determine how each model parameter affects space suit component flexibility in bending. Bending tests on a variety of simple cylindrical joint mockups are then performed to verify the strategies for joint flexibility that are indicated by the model. Then these strategies are applied to the more complex geometry of the glove metacarpophalangeal (MCP) joint in an attempt to improve the flexibility of that joint.

Model Development

The purpose of this section is to develop a model of a pressurized fabric structure that can be used to gain insight into the mechanisms governing stiffness and mobility in space suits. Little modeling work has been done to date on fabric structures, because they have some unusual characteristics that make predicting their behavior something of a challenge. Chief among these are the fact that fabric is an inherently highly nonlinear and anisotropic material: though it can carry loads in tension, it wrinkles and collapses when it is subjected to compressive loads. Also, because of the square weave pattern of the fabric, it has distinctly different moduli depending on the weave direction examined.

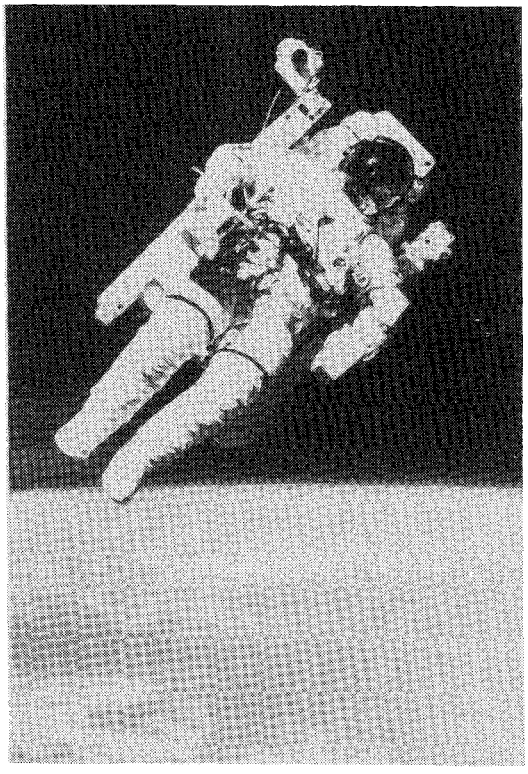

Fig. 1 Photograph of the current NASA Shuttle space suit (courtesy ILC Dover, Inc.).

Fabric Modeling

Weave directions in a fabric are defined by the way the fabric comes off the loom (see Fig. 2). The direction of thread travel through the loom is known as the warp direction. These threads are placed in tension by the loom during the weaving process and will travel the complete length of the bolt of cloth. The fibers that are oriented 90 deg off the warp direction are called the fill fibers (or weft, or woof). These threads are woven perpendicularly through the warp threads as they travel through the loom. Typically the tensile modulus of the fabric in the fill direction (E_f) is less than the tensile modulus in the warp direction (E_w).

The differences in moduli in the warp and fill directions may be accommodated by modeling the fabric as an orthotropic membrane with the following constitutive relationships[6]:

$$\varepsilon_w = \frac{N_w}{E_w} - \frac{\nu_w N_f}{E_w} \tag{1a}$$

$$\varepsilon_f = \frac{N_f}{E_f} - \frac{\nu_w N_w}{E_w} \tag{1b}$$

$$\gamma_{wf} = \frac{N_{wf}}{G} \tag{1c}$$

$$\frac{\nu_w}{E_w} = \frac{\nu_f}{E_f} \tag{1d}$$

The fabric is considered to be in an unstrained state after glove construction but before glove donning or pressurization.

EVA Glove Geometry

Because of the complexity involved in dealing with the wrinkling behavior of pressurized fabric structures, it is beneficial to simplify the structural geometry of the component in question as much as possible, but not so much that applicability to the problem is lost. For example, examination of the pressurized space-suit glove shows that the region surrounding the MCP joint can be approximated by an inflatable fabric tube subjected to a bending moment from the hand (see Fig. 3). It is further assumed that the principal weave directions of the fabric used in the glove construction correspond to

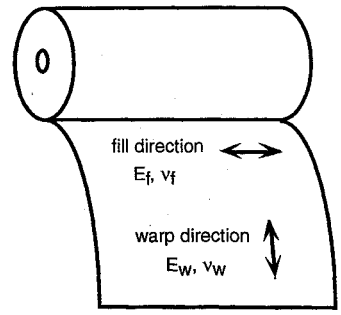

Fig. 2 Sketch showing the warp and fill directions on a bolt of fabric.

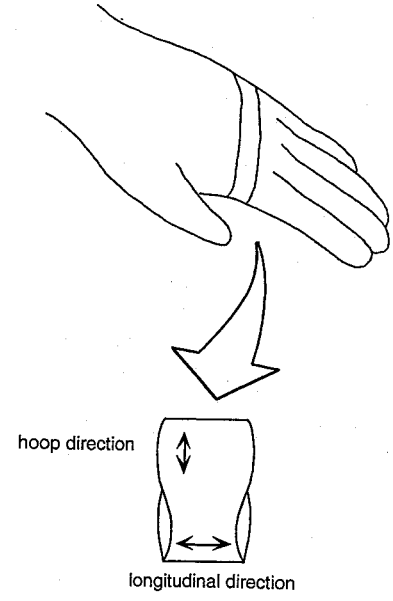

Fig. 3 Sketch of the pressurized-fabric-tube analogy for the EVA-glove MCP joint.

the longitudinal and hoop directions of the fabric tube. Other suit elements that can be approximated by pressurized fabric tubes subject to bending moments include the arm components, leg components, and glove fingers.

Suit pressurization alone causes two types of loading on the suit fabric at the MCP joint: a hoop-type stress that travels around the glove cross section, and a longitudinal stress perpendicular to the hoop stress. A bending moment that is applied by the enclosed hand to the glove section will cause an additional task-induced longitudinal load in the fabric and cause a curvature of the glove. As the applied moment from the hand increases, the glove will go through two distinct states as it bends: one where the moment is small and no wrinkling is evident, and one where wrinkling has begun on the palm and is spreading around the glove. In the taut stage of the bending process, or where the longitudinal stresses in the glove section remain tensile around the complete circumference, the longitudinal stress distribution illustrated in Fig. 4 is assumed for the fabric.

In this stage the value of the longitudinal stress resultant N_l in the glove fabric is defined as

$$N_l = N_{l0}\left(\frac{1+\cos\theta}{2}\right) + N_{lm}\left(\frac{1-\cos\theta}{2}\right) \tag{2}$$

where N_{l0}, N_{lm}, and θ are defined in Fig. 4.

As the applied moment on a section of the glove increases, the bending stress equilibrates the longitudinal stress in the fabric skin on the palmar side of the glove, and wrinkling begins in that region. Since the glove fabric is subjected to a biaxial stress field, the longitudinal stress is not necessarily zero when the longitudinal strain is zero. Wrinkling begins when the strain, not the stress, drops below

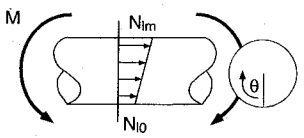

Fig. 4 The assumed stress distribution in the fabric of the EVA-glove MCP joint when no wrinkling is present.

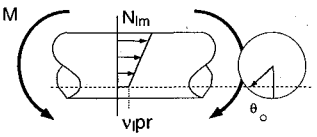

Fig. 5 The assumed stress distribution in the fabric of the EVA glove when wrinkling occurs on the palm.

zero. Using this result and solving Eq. (1a) for N_l when $\varepsilon_l = 0$ yields

$$N_l = \nu_l N_h \tag{3}$$

For a glove metacarpophalangeal joint, with a cylindrical cross section and the longitudinal and hoop directions defined as shown in Fig. 3, N_h is a simple hoop stress, and the minimum stress in the longitudinal direction that is necessary to prevent wrinkling becomes

$$N_l = \nu_l pr \tag{4}$$

where p is the internal pressure and ν_l is the Poisson's ratio of the fabric. Thus the longitudinal stress below which the fabric can carry no tensile load is $\nu_l pr$, and the stress distribution in the wrinkled region is assumed to take the form shown in Fig. 5.

For the partially wrinkled state the stress resultant in the longitudinal direction illustrated in Fig. 5 can be expressed as

$$N_l = \begin{cases} \dfrac{(\cos\theta_0 - \cos\theta)(N_{lm} - \nu_l pr)}{1 + \cos\theta_0} + \nu_l pr & \text{for} \quad \pi > \theta > \theta_0 \\ N_l = 0 & \text{for} \quad \theta_0 > \theta > 0 \end{cases} \tag{5}$$

The balance of moments about a transverse axis through the center of the glove section is expressed as

$$M = -2\int_0^{\pi} N_l r^2 \cos\theta \, d\theta \tag{6}$$

where M is the moment applied to the glove cross section. When no wrinkling is present around the circumference of the MCP joint, Eqs. (2) and (6) can be combined to give

$$N_{lm} - N_{l0} = \frac{2M}{\pi r^2} \tag{7}$$

The curvature of the joint cross section in the unwrinkled state is given by

$$K = \frac{N_{lm} - N_{l0}}{2E_l r} \tag{8}$$

where $K = 1/\rho$, ρ being the resulting radius of curvature of the section. Substitution of Eq. (7) into Eq. (11) yields

$$K = \frac{M}{\pi r^3 E_l} \tag{9}$$

When wrinkling is present in the palm of the glove, Eq. (5) is substituted into Eq. (6) to perform the balance of moments. This yields

$$N_{lm} = \frac{(M - 2\nu_l pr^3 \sin\theta_0)(1 + \cos\theta_0)}{r^2[(\pi - \theta_0) + \sin\theta_0 \cos\theta_0]} + \nu_l pr \tag{10}$$

The balance of longitudinal forces on the glove cross section reduces to

$$p\pi r^2 = 2\int_0^{\pi} N_w r \, d\theta \tag{11}$$

The longitudinal force balance on the wrinkled glove joint is performed by substituting Eq. (5) into Eq. (11):

$$N_{lm} = \frac{pr[\pi - 2\nu_l(\pi - \theta_0)](1 + \cos\theta_0)}{2[(\pi - \theta_0)\cos\theta_0 + \sin\theta_0]} + \nu_l pr \tag{12}$$

Equating the expressions for N_{lm} in Eqs. (10) and (12) yields the following expression that relates the wrinkle angle to the applied moment:

$$\frac{M}{pr^3} = \frac{(\pi/2)[(\pi - \theta_0) + \sin\theta_0 \cos\theta_0]}{\sin\theta_0 + (\pi - \theta_0)\cos\theta_0} - \frac{\nu_w\left[(\pi - \theta_0)^2 - (\pi - \theta_0)\sin\theta_0 \cos\theta_0 - 2\sin^2\theta_0\right]}{\sin\theta_0 + (\pi - \theta_0)\cos\theta_0} \tag{13}$$

Substitution of $\theta_0 = 0$ into Eq. (13), when wrinkling is just beginning on the palm of the glove, shows that the magnitude of the applied moment at the inception of wrinkling is

$$|M_{\text{wrinkle}}| = \frac{\pi pr^3}{2}(1 - 2\nu_l) \tag{14}$$

The curvature of a wrinkled-glove-joint cross section is given by

$$K = \frac{N_{lm} - \nu_l pr}{E_l r(1 + \cos\theta_0)} \tag{15}$$

Substituting Eq. (12) into this expression yields

$$K = \frac{M - 2\nu_l pr^3 \sin\theta_0}{E_l r^3[(\pi - \theta_0) + \sin\theta_0 \cos\theta_0]} \tag{16}$$

The complete moment-curvature relationship for the simplified glove joint cross section can now be expressed as

$$K = \frac{M}{E_l \pi r^3} \quad \text{for} \quad M < \frac{\pi pr^3}{2}(1 - 2\nu_l) \tag{17}$$

$$K = \frac{M - 2\nu_l pr^3 \sin\theta_0}{E_l r^3[(\pi - \theta_0) + \sin\theta_0 \cos\theta_0]} \quad \text{for} \quad M > \frac{\pi pr^3}{2}(1 - 2\nu_l) \tag{18}$$

The relationship between the moment applied to the glove by the hand and the curvature caused by that moment can be examined by solving the above system of equations. While the structure remains unwrinkled, the bending behavior of the tube is simply described by Eq. (17). When the applied moment exceeds the wrinkling threshold, Eq. (13) must be used to determine the appropriate wrinkle angle for the applied moment before determining the curvature of the structure using Eq. (18).

It is important to note that the analysis was performed under the assumption that the moment M will have a negative sign. If the analysis is performed assuming a positive moment, the sign in the numerator in Eq. (18) will change to a positive one.

Simulations

The model embodied in Eqs. (17) and (18) was used to generate the plots in Fig. 6 that show the moment applied to the glove as a function of glove bending curvature. Each plot displays an identical moment-curvature curve using nominal values for each of the model parameters ($p = 50{,}000$ Pa, $r^3 = 3.2 \times 10^{-5}$ m^3, $E_l = 80{,}000$ N/m, $\nu_l = 0.250$). The plots also display curves showing the effects of a $\pm 50\%$ variation in each model parameter.

Each curve has three characteristics that should be noted for comparison. The initial linear portion of each moment-curvature plot reflects the bending of the cross section before any wrinkling occurs

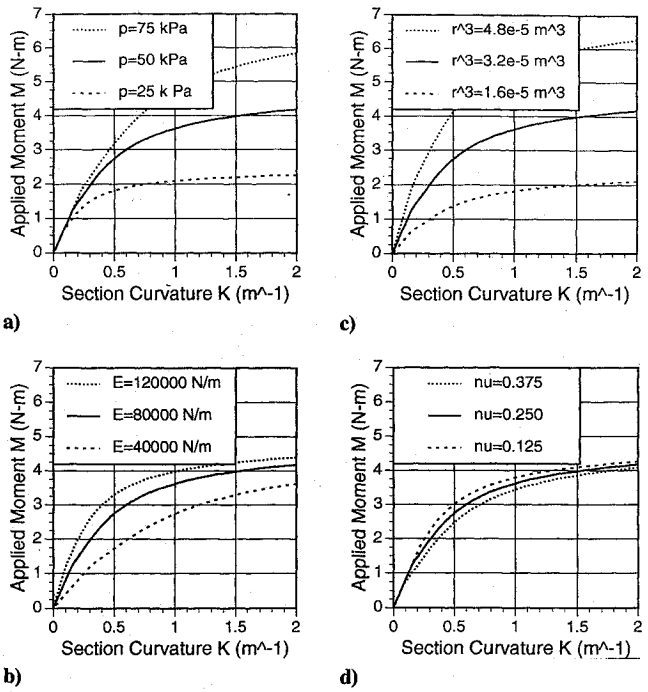

Fig. 6 Effects of various parameters on the relation between applied moment and glove bending curvature.

and has a slope of $\pi r^3 E_l$. The departure of the curve from the linear portion of the graph predicts the beginning of wrinkling on the palmar side of the glove. The departure begins when the magnitude of the moment exceeds $\pi p r^3(1 - 2\nu_l)/2$ and represents a gradual decrease in the stiffness of the glove as wrinkles propagate around the circumference of the glove. The moment-curvature plots then converge to the maximum bending resistance of the glove section, equal[7] to $\pi p r^3$.

Effect of Glove Pressurization

Figure 6a illustrates the effect that pressurization level has on glove stiffness. Moment-curvature plots are shown for a glove pressurized to three different levels: $p = 25$, 50, and 75 kPa. The model shows that pressurization has little effect in the initial nonwrinkled state, but dramatically effects the postwrinkling behavior of the glove. Raising glove pressure raises the required wrinkling moment, delaying the improved flexibility that wrinkling provides, although it should be noted that wrinkling may be detrimental to palm tactility. The internal pressure level is also directly proportional to the maximum bending resistance of the glove MCP joint, so an increase or decrease in pressure induces a proportional increase or decrease in the ultimate resistance of the glove.

Obviously, in the interest of glove flexibility, the suit pressure should be kept as low as possible; however, the overwhelming considerations that define the suit internal pressure are not mobility and dexterity, but the physiological needs of the astronaut, specifically the need to minimize both prebreathing time and the risk of aeroembolism. The current trend in space-suit design is for an increase in suit pressure in the next generation of space suits.[3] This increase will have a significant detrimental effect on the flexibility of the glove, so opportunities to improve glove mobility by other means should be thoroughly investigated.

Effect of Glove Size

Figure 6b shows the effect of a ±50% variation in glove size (reflected in the quantity r^3) on the glove moment-curvature relationship. The smaller glove cross section dramatically improves the bending characteristics of the glove through a lower stiffness in the straight-line section of each curve, a lower wrinkling moment, and a significantly lower maximum glove resistance.

Much of the current research on glove improvement focuses on creating closer-fitting and thus smaller, more flexible gloves. The model presented in this paper supports the need for this research by demonstrating the dramatic effect that glove size has on the applied moment-bending curvature relationship. There is no real drawback to improving glove mobility through a better-fitting and smaller glove, but the obvious limit on this strategy is the size of the hand itself.

Effect of Fabric Mechanical Properties

As discussed above, both internal pressurization and glove size are dominant factors in glove mobility. However, the glove pressure is almost completely out of the control of the glove designer, and the potential for improvement of glove mobility through size reduction is limited by the size of the hand. This leaves the mechanical properties of the fabric, Young's modulus and Poisson's ratio, as the most promising areas for further improvement in glove mobility.

The effects of changes in the longitudinal modulus E_l and Poisson's ratio ν_l are illustrated in Figs. 6c and 6d. While E_l does not affect the wrinkling moment or the maximum glove resistance, it does change the slope of the moment-curvature relationship in both the wrinkled and unwrinkled portions of the plot. In other words, a reduction in longitudinal fabric modulus is reflected by a proportional drop in glove stiffness. The effects of reducing the fabric modulus are not as dramatic as those of reducing glove size or pressurization, but fabric modulus is the one largely unexplored area that can still yield significant improvement in glove mobility. Improvement in this fashion may not come without cost, however. As the fabric modulus decreases, the challenge of making a close-fitting glove will become even greater.

Figure 6d illustrates a strategy for improving glove mobility that has no readily apparent drawbacks. In this plot the Poisson's ratio of the fabric is varied to demonstrate the effect it has on the bending stiffness of the glove. The principal effect that ν_l has is on the moment required to cause wrinkling on the palm of the glove. The simulation demonstrates that as ν_l increases the wrinkling moment drops. This causes the decrease in glove stiffness brought on by the wrinkling of the fabric to occur at a much smaller applied moment. In fact, if $\nu_l > 0.5$ the fabric will wrinkle with any application of bending moment from the hand. The gain in glove flexibility with this strategy is small, but it is without obvious penalty. All that is required is to choose from the set of currently available glove materials those which have the highest Poisson's ratio.

Verification of Improved Flexibility Joint Strategies

The strategies outlined in the previous section for improving glove flexibility can be separated into the two categories of "design" methods and "materials" methods. The design parameter that is included

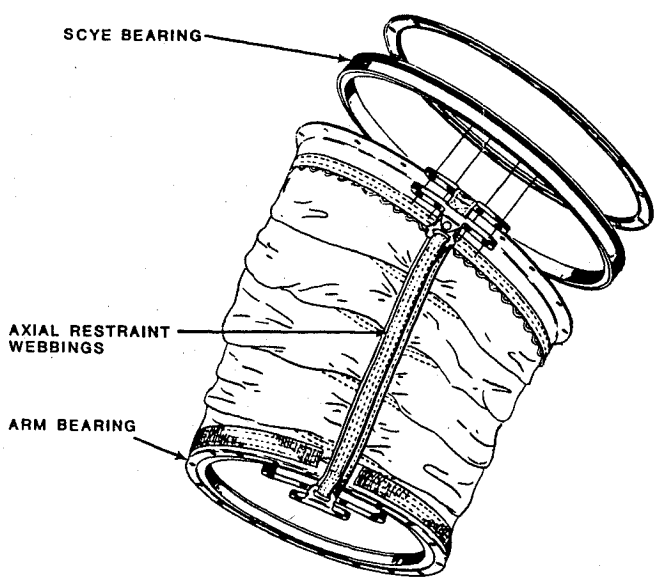

Fig. 7 Detailed sketch of the upper-arm fabric convolute joint from the Shuttle space suit (courtesy ILC Dover, Inc.).

in the bending model developed here is the quantity r^3. The value of this quantity was varied in Fig. 6a to show the effect of glove size on bending stiffness. This simple simulation illustrated the dramatic effect that this term has on stiffness, but treating r^3 as merely a size term ignores its true significance. Examining Eq. (17) again and making the substitution $I = \pi r^3$ results in an expression that is identical to the curvature expression for a solid elastic beam, where M is the applied moment, E_l the material modulus, and I the moment of inertia:

$$K = \frac{M}{E_l I} \tag{19}$$

The only difference is that in the case of the pressurized space-suit joint the material modulus is expressed as load per unit width, so the resulting moment of inertia is expressed in terms of length cubed.

Using this beam analogy for the bending behavior of fabric space-suit joints is very useful, because it allows the application of experience with a wide variety of elastic beam bending problems to the rather more unusual problem of stiffness in soft-goods space suits. The beam analogy shows that suit flexibility can be improved not only by reducing the size of the joint, but also by lowering the member moment of inertia. This can be accomplished with two simple steps: minimize the amount of material that carries the longitudinal load in the joint, and keep the remaining material as close as possible to the neutral bending axis. This idea has been in use for some time and is well illustrated by the fabric convolute joints used in the upper-arm, finger, and knee components of the current NASA space suit (see Fig. 7).[5] Typically these fabric convolutes consist of a series of folds around the joint so there is ample material for the outside of the joint to elongate as it bends. Heavy webbing is sewn into the sides of the convolute to carry the longitudinal pressurization and task-induced loads and to keep the convolute from expanding uncontrollably. Since the longitudinal load is carried only by the webbing at the sides of the joint, the moment of inertia and thus the bending stiffness of the suit is significantly decreased. This design has been quite successful when the geometry of the suit surrounding the joint is generally cylindrical.

The material parameters in fabric space-suit joint design are, of course, E_l and ν_l. Strategies for improving glove flexibility through material selection are well illustrated in Figs. 6c and 6d and were sufficiently discussed in the previous section. What is important to note, however, is that a reduction in longitudinal material modulus will improve joint flexibility even if the joint is not a simple tube as the model assumes. The model indicates that joint flexibility is a function of both the moment of inertia and the material properties. This means that, even if the joint has a modified design like a fabric convolute, further gains in flexibility can be made if the material properties are manipulated, particularly if the modulus of the remaining fabric carrying the longitudinal load is reduced.

A series of tests was performed to demonstrate this idea. A bending apparatus was constructed so that various cylindrical suit-element mockups could be pressurized and bending-moment–deflection relationships determined. Figure 8a shows the test apparatus during a bending test of a simple fabric tube. The protocol required deflecting the test specimen in 5-deg increments up to 90 deg by pulling a small handle attached to the end of the movable arm. A load cell mounted between the handle and the tube fixture allowed the bending moment at each deflection to be calculated. Each 0–90-deg bending test was repeated 10 times.

Three different 6-cm-diam joint mockups were tested: the simple tube shown in Fig. 8a and two fabric convolute joints. These are shown in Figs. 8b and 8c. The two fabric convolutes differ only in the structure that carries the longitudinal pressurization load. With the simple fabric tube, of course, the longitudinal load is evenly distributed around the complete circumference when undeformed. In the convolute shown in Fig. 8b the longitudinal load is borne by a single strand of nylon cord that is wound through grommets in the seam that protrudes on each side of the joint. The modified convolute joint shown in Fig. 8c uses the same cord, but winds it around a block of soft rubber as it travels the length of the joint. This lowers the effective modulus (or spring constant) of the cord, since the cord will compress the rubber, thus elongating the entire assembly, as the longitudinal stresses increase due to bending. Tests showed that the spring constant of the cord alone was approximately 81 N/cm and the spring constant of the cord-rubber assembly was 49 N/cm.

The results of the bending tests are shown in Fig. 9. The error bars on each point represent the 99% confidence interval de-

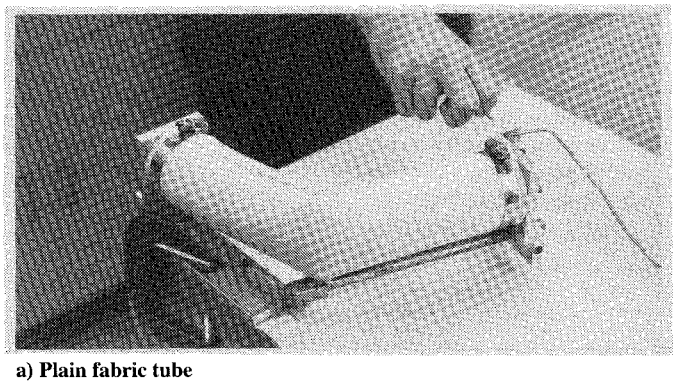

a) Plain fabric tube

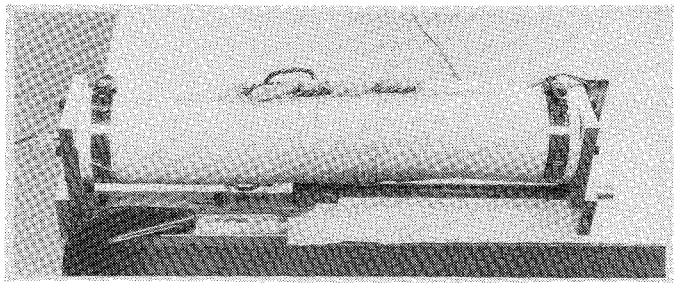

b) Fabric convolute with nylon cord axial restraint

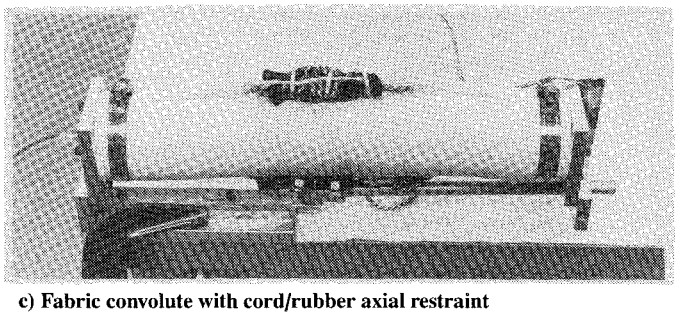

c) Fabric convolute with cord/rubber axial restraint

Fig. 8 Photos of the cylindrical joint mockups mounted in the bending apparatus.

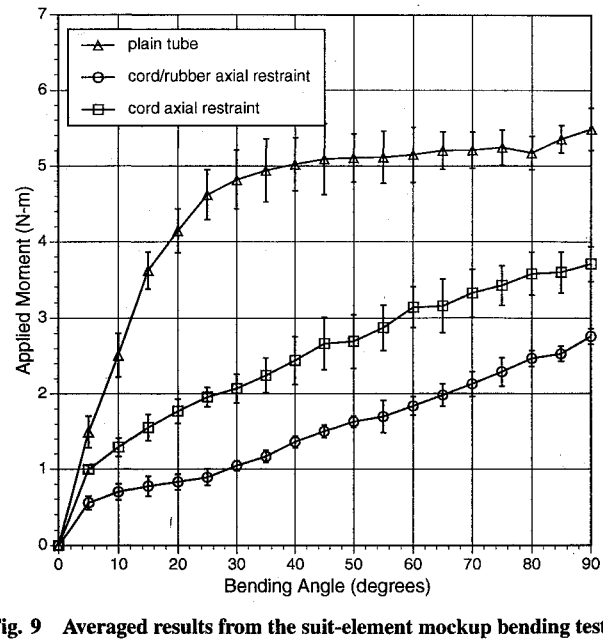

Fig. 9 Averaged results from the suit-element mockup bending tests.

termined from the experimental data. The bending test of the plain fabric tube demonstrated that it made the stiffest joint of those tested. Note that the shape of the curve is very similar to those shown in the model bending simulations. Also shown on this plot are the results of the bending tests of the two-fabric convolute joints. As expected, the reduction in moment of inertia that was achieved by replacing the plain fabric tube with the fabric convolute lowered the stiffness of the joint dramatically. Further tests showed that replacement of the high-modulus cord with the lower-modulus cord-rubber longitudinal-load-carrying assembly reduced the stiffness of the joint even more. This shows that improvement in joint flexibility is possible by lowering the modulus (or spring constant) of the portion of the joint carrying the longitudinal load, regardless of the design details of the joint itself.

Metacarpophalangeal-Joint Design for a Space-Suit Glove

The major point to be gleaned from the previous sections is that the modulus of the material used in the construction of a space-suit glove is as important a consideration for glove flexibility as size and design. The tests described in the previous section demonstrated that both design changes and material changes significantly effect the stiffness of a joint with cylindrical geometry. However, designs like the fabric convolute are not feasible if the geometry of the joint is not cylindrical, so concepts that concentrate on changing the material properties of the joint may be the solution in these cases. An excellent example of such a joint is the MCP joint for a space-suit glove.

The MCP joint presents unusual difficulties because of the flat geometry of the palm and the back of the hand. Flat surfaces in inflated structures are difficult to create using only soft goods, because the structure will wrinkle and deform to minimize the stresses in the fabric. Lowering stresses in pressurized structures is achieved by reducing the radius of curvature of the structure surface. This means that flat surfaces tend to assume cylindrical or spherical shapes due to the internal pressurization.[8] This tendency for flat surfaces to become curved precludes the use of a fabric convolute on the back of the hand to improve mobility, since the convolute will simply expand upon pressurization from the initially flat configuration to lower the fabric stresses. The obvious alternative strategy is to manipulate the material properties of the glove to improve joint mobility.

A unique glove was designed and constructed specifically for testing this concept. This glove was designed to embody as many of the features of the current space-suit glove as possible. Shown in Fig. 10, the test glove consists of a fabric restraint layer over a latex inner glove. The glove includes a palm bar to prevent ballooning, a strap over the back of the hand to further tighten the glove over the palm at the MCP joint, and fabric convolute finger joints for finger mobility. An important feature unique to this glove is the inclusion of a large pleat that extends from the edges of the palm over the knuckles on the back of the hand. This pleat gives the glove a pressurized neutral position with the fingers flexed approximately 60 deg toward the palm at the MCP joint while retaining a close circumferential fit.

The glove was designed to accept three distinct dorsal assemblies which change the spring constant of the longitudinal-load-bearing structure of the MCP joint. These assemblies are mounted on the glove at attachment points at the base of each finger and a large Velcro® mount on the glove wrist. Each assembly has the effect of pulling the neutral position of the glove fingers back to a zero flexion angle. These dorsal assemblies act to carry the longitudinal pressurization and task-induced stresses in the back of the glove while the hoop stresses are still borne by the underlying fabric. In this way the glove remains tight-fitting, avoiding one of the pitfalls of lowering the fabric modulus. The simplest of the three dorsal assemblies is a panel of fabric that attaches to the wrist and is laced into the finger attachment points. This version is considered the standard version and is intended to be analogous to a pressurized space-suit glove without any MCP joint modifications.

a) Plain fabric panel

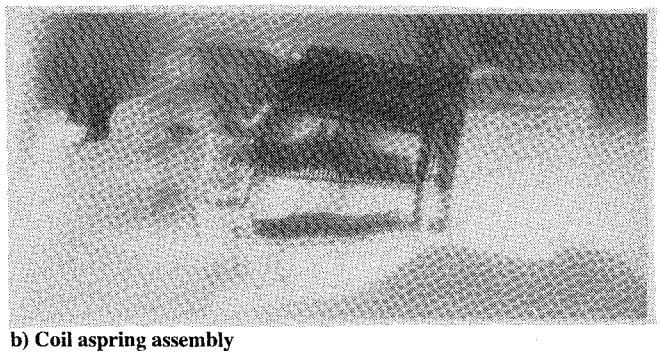

b) Coil aspring assembly

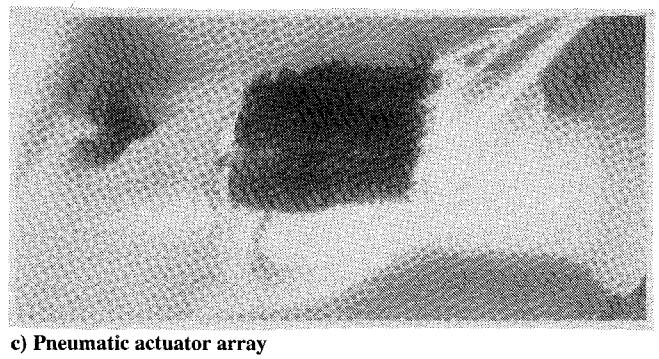

c) Pneumatic actuator array

Fig. 10 Photographs of the different types of glove MCP joints tested in the evacuated glove box.

A coil-spring dorsal assembly was also constructed and represents an attempt to increase MCP joint flexibility by lowering the spring constant of the longitudinal load-bearing structure on the back of the glove in a very definable fashion. The springs chosen for this assembly (SPEC Model E0360-039-2000, $k = 0.508$ N/mm, free length = 50.8 mm, diameter = 9.14 mm) have a spring constant that is significantly lower than that of the fabric panel in the standard version.

A pressurized-gas-powered space suit glove was also constructed that replaces the fabric panel of the standard version with an array of four pneumatic actuators. Adding these actuators to the dorsal portion of the EVA glove mockup provides control over the neutral position of the glove fingers, effectively changing the modulus of the dorsal portion of the glove through the addition of an active subsystem. Each actuator consists of a 6-cm-long, 1.5-cm-diam neoprene tube inside a 12-cm-long, 1.5-cm-diam rip-stop nylon sleeve. The ends of both the neoprene tube and the nylon sleeve are tightly bound to a brass plug on each end of the actuator with whipping cord. The brass plugs also serve as the points for attachment of the actuator to the glove and for connection of the gas supply. The restrictive diameter dimension and the generous length dimension of the nylon sleeve cause the neoprene tube and therefore the actuator to lengthen considerably without expanding radially as the tube is pressurized. The neoprene tubes enclosed in the nylon sleeves have a spring constant that is approximately the same as that of the coil springs in the previously described coil-spring dorsal assembly. Mounting an array of these actuators on the back of the test mockup

Table 1 Pneumatic-actuator controller truth table

Sensor output	Exhaust valve	Pressure valve
$< V_e$	Open	Closed
$> V_e$ and $< V_p$	Closed	Closed
$> V_p$	Closed	Open

acts to pull the neutral position of the fingers back to a zero flexion angle because of the tensile load-carrying ability of the neoprene tube. There is the added ability, however, to manipulate the load-deflection behavior of the back of the glove by pressurizing and exhausting the actuators.

Finger independence and dexterity are preserved by providing each finger actuator with an independent gas flow control system. The actuators are each controlled with an independent sensor and control circuit using measurements of the glove-finger contact pressure obtained from a thin pressure sensor placed between the hand and the glove on the palmar face of the first phalanx at the base of each finger. The sensors consist of a layer of polyester film with a thin layer of ink screened on the surface. The resistivity of the ink is pressure-dependent, so that an extremely thin pressure sensor could be fabricated by covering the ink patch with another layer of polyester film and measuring the resistance change of the ink with a bridge circuit. The sensor has a thickness of 0.15 mm. After lead attachment and application of a protective layer of insulating tape, the sensor assembly has a thickness of 0.51 mm.

A simple threshold control system was breadboarded for tests of the pneumatic gloves. It uses the voltage output of each finger sensor to decide whether the actuator on that finger should pressurize, exhaust, or take no action. The control strategy is shown in Table 1. As the hand moves against the glove, no action is taken by the control system until an upper pressure threshold V_p is exceeded. At this point the pressurization valve opens and the actuator fills and lengthens, changing the geometry of the glove and allowing the finger to flex. The actuator extends to the point that the pressure between the hand and glove is reduced below the threshold V_p, closing the pressurization valve. As long as the voltage output remains between V_p and the exhaust threshold V_e, no action is taken by the control system. When the hand extends back toward neutral position, the pressure sensor reading will drop further and go below V_e. In this region the controller opens the exhaust valve.

Bending Tests of Experimental MCP Joints

All tests were performed in a glove box that was constructed specifically for this study. This equipment allows tests of space-suit glove prototypes in an environment similar to that found in space. The glove box can be evacuated down to 827 kPa (12 psi) below atmospheric pressure to simulate the pressure difference across the space suit. In all of the tests discussed here the box was evacuated to 414 kPa (6 psi). Tests of all three glove embodiments consisted of a series of 90-deg flexions of all four fingers. The test subject was instructed to perform a series of 10 flexion tasks at three different rates: 5, 2, and 1 s/cycle. The data from the first five tasks were discarded to allow time for glove settling and task familiarization. All the data presented here were collected from tasks 6–10. Pressure data from the sensor mounted at the base of the first finger were recorded during the tests of each joint version and are the basis for the joint stiffness comparisons.

Tests of the glove with the pneumatic actuator assembly required setting the pressurization and exhaust thresholds prior to the test. For the data presented here V_p and V_e were set to correspond to 42.9 and 24.5 kPa on the sensor calibration curve.

A summary of the peak pressures measured between the base of the first finger and the glove for the standard, coil spring, and adaptive glove versions is included as Fig. 11 with the 90% confidence interval displayed for each data point. The average maximum finger pressure in the standard glove was the highest at all three flexion rates: 155.6, 142.61, and 135.31 kPa for the 1-, 2-, and 5-s tests, respectively.

The coil-spring glove, with an effective modulus that was lower than in the standard version, showed improved joint flexibility, with

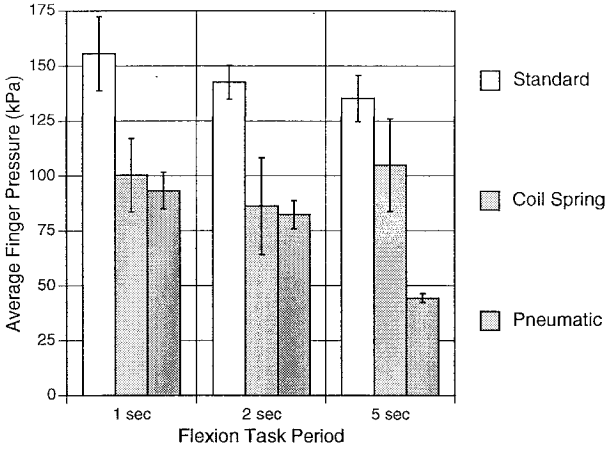

Fig. 11 Chart showing the average finger pressures measured between the hand and each glove version during 90-deg finger flexion tasks.

average peak finger pressures measuring 100.26, 86.18, and 104.86 kPa in the 1-, 2-, and 5-s tests, respectively. This is an average reduction in finger pressure of 32.6%.

The results of the pneumatic-actuator glove tests varied across the range of finger flexion rates. In the 1-s-cycle test the average peak pressure of 93.22 kPa measured between the hand and the glove represented a 40.0% drop from the standard glove in the same test. During the 2-s-cycle tests the average peak pressure in the pneumatic glove was found to be 82.26 kPa, a 41.6% improvement over the standard. The results improved even more in the 5-s-cycle test, when the average peak finger pressure was found to be 44.37 kPa, a 67.2% improvement over the standard.

In the tests of the pneumatic glove system there is an evident rate dependence in the results. The rate of extension of the actuator, and thus the rate of change of the neutral angle of the glove finger, is determined by the mass flow rate of the gas into the actuator. It is obvious from the experimental data that as the flexion rate increased the flow rate of the gas was not sufficient to keep the neutral angle of the glove finger moving at the same rate as the finger itself. This resulted in higher finger pressures in the pneumatic glove at higher flexion rates. In all cases, however, the finger pressures measured in the pneumatic glove were lower than those in the standard glove, indicating a corresponding reduction in joint stiffness and hand fatigue.

The main conclusion that should be drawn from this series of tests is that, as indicated by the structural model, the modulus of the load-carrying structure does have a direct and dramatic effect on hand mobility in the space-suit glove. The operational requirements on the gloves have resulted in a durable glove, which is constructed of robust fabric. This fabric has a high modulus to prevent excessive expansion when pressurized. This high modulus is detrimental to the glove's flexibility, however. The tests performed in this study show that lowering the effective modulus of the glove fabric either through passive or active schemes reduces bending stiffness significantly and that fabric modulus should be an important consideration when choosing candidate materials for future space suits.

Both the coil-spring assembly and the pneumatic-actuator assembly demonstrated a marked improvement in MCP joint flexibility. While it appears from the experimental data that the pneumatic-actuator assembly has the greater potential for improving joint flexibility, this method has the rather serious drawback of requiring a pressurized gas source and control hardware and electronics. This will add weight and complexity to the space suit.

The results of the coil-spring assembly test demonstrate a more practical way to improve joint mobility. Since the joint is made up of passive mechanical components, there is no additional power or control hardware to be concerned about. There is also great flexibility in a concept such as this, because it does not matter what the structure on the longitudinal-load-bearing portion of the glove is made up of as long as it has a low effective modulus. Alternatives that could potentially achieve the same effect as the coil springs

Table 2 Overview of EVA-glove mobility factors

Glove mobility factors	Constraints	Current direction
Suit pressurization (p)	Dictated by physiological requirements: Higher pressure lessens probability of aeroembolism.	↑ (detrimental to glove mobility)
Glove fit (r^3)	Design and construction skill of glove vendors; utilization of new technology.	↓ (improving glove mobility)
Fabric modulus (E)	Ability of glove vendors to construct a glove from lower-modulus materials and keep it close-fitting.	? (lower modulus improves glove mobility)
Fabric Poisson's ratio (ν)	No obvious constraint.	? (higher ν improves glove mobility)

used in this study are fabric panels, linkage mechanisms, or other types of springs such as constant-force springs.

Conclusions

The structural model developed in this paper identifies four factors as directly influencing the bending characteristics of the space-suit components. These are suit pressurization, glove fit, fabric modulus, and fabric Poisson's ratio (Table 2). Of these, the glove pressurization level is out of control of the glove designer, and improving glove fit is already a focus of current research efforts. This leaves the mechanical properties of the fabric as the only uninvestigated candidates for future research in improving glove mobility. Tests on cylindrical joint mockups and space-suit glove mockups also indicated that manipulating the mechanical properties of the glove fabric can improve glove mobility.

One possible solution to this problem is the creation of a class of materials specially woven for space-suit glove use (Fig. 12). This material would have an extremely high modulus in the hoop direction of the MCP joint, where the loads are principally pressurization loads, to keep the fabric from stretching and ballooning away from the palm as the suit is pressurized. In the longitudinal direction, where the task-induced loads from finger flexion are carried, the modulus would be kept as low as possible to reduce joint stiffness, and the Poisson's ratio maximized to encourage wrinkling and the improved mobility that it brings. A simpler method of accomplishing this same goal is to use separate fabric layers to achieve the same results; a high-modulus layer to carry the hoop pressurization loads, and a low-modulus layer to carry the longitudinal pressurization and task-induced loads. Radically changing the material properties of the glove fabric will require modifications of the sizing procedures and glove designs used by the glove manufacturers. Obviously, if a smaller-modulus material is used, the fabric will stretch more when the suit is pressurized.

Currently fabrics for space-suit gloves are chosen primarily for their ability to protect the wearer and for ease of glove construction. This research indicates that the material properties of the fabric should be an important consideration in the fabric selection process, since it directly and dramatically affects the stiffness of the gloves. Included in this work is a simulation procedure that can be used to determine which fabrics have the best qualities for use in space-suit gloves by providing the lowest stiffness joint.

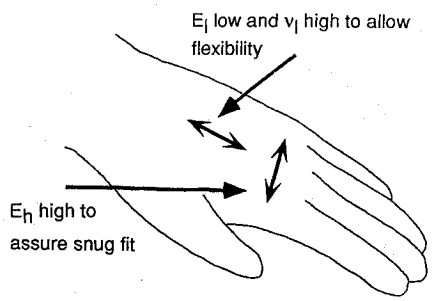

Fig. 12 Sketch of an EVA glove with the recommendations on fabric mechanical properties indicated by the pressurized-fabric-tube model.

Acknowledgments

The authors wish to thank the NASA Office of Advanced Concepts and Technology and the NASA National Space Grant College and Fellowship Program for their support of this research. Portions of this research were presented at the 22nd International Conference on Environmental Systems in Seattle, Washington, July 13–16, 1992.

References

[1]Mallan, L., *Suiting Up for Space*, 1st ed., John Day, New York, 1971, pp. 187–220.

[2]O'Hara, J. M., Briganti, M., Cleland, J., and Winfield, D., "Extravehicular Activities Limitations Study Volume II: Establishment of Physiological and Performance Criteria for EVA Gloves," NASA CR-172099, 1988.

[3]Kosmo, J., Bassick, J., and Porter, K., "Development of Higher Operating Pressure Extravehicular Space-Suit Glove Assemblies," Society of Automotive Engineers, Paper 881102, July 1988.

[4]Spampinato, P., Cadogan, D., McKee, T., and Kosmo, J., "Advanced Technology Application in the Production of Spacesuit Gloves," Society of Automotive Engineers, Paper 901322, July 1990.

[5]Balinskas, R., McBarron, J., and Spampinato, P., "Shuttle Extravehicular Mobility Unit (EMU) Operational Enhancements," Society of Automotive Engineers, Paper 901317, July 1990.

[6]Firt, V., *Statics, Formfinding and Dynamics of Air-Supported Membrane Structures*, 1st ed., Martinus Nijhoff, The Hague, 1983, pp. 166–178.

[7]Bulson, P. S., "Design Principles of Pneumatic Structures," *The Structural Engineer*, Vol. 51, No. 6, 1973, pp. 209–215.

[8]Otto, F., *Tensile Structures*, 1st English ed., Vol. 1, MIT Press, Cambridge, MA, 1967, pp. 10–69.